JOURNAL OF NANO- AND ELECTRONIC PHYSICS *ЖУРНАЛ НАНО- ТА ЕЛЕКТРОННОЇ ФІЗИКИ*
Vol. **12** No 3, 03011(5pp) (2020) Том **12** № 3, 03011(5cc) (2020)

Investigation on Electrical and Structural Properties of Manganese Dioxide Nanoparticles

S.C. Vella Durai[1], E. Kumar[2], D. Muthuraj[3], V. Bena Jothy[4]

[1] *Department of Physics, JP College of Arts and Science, Agarakattu, Tenkasi, Tamilnadu, India*
[2] *School of Science, Department of Physics, Tamil Nadu Open University, Chennai. Tamilnadu, India*
[3] *PG and Research Department of Physics, The M.D.T Hindu College, Tirunelveli. Tamilnadu, India*
[4] *Department of Physics & Research Center, Women's Christian College, Nagarcoil. Tamilnadu, India*

(Received 08 January 2020; revised manuscript received 15 June 2020; published online 25 June 2020)

Crystalline manganese dioxide (MnO_2) was prepared by microwave assisted solution method using sodium hydroxide as an agent. Electric conductivity, electric modulus and dielectric properties of MnO_2 nanoparticles were analyzed by AC Impedance spectroscopy in the frequency range 1 to 8 MHz and temperature range in-between 273 K to 423 K. Conductivity of MnO_2 increases with increasing frequency. Temperature dependence of the nanoparticle conductivity was found to obey the Arrhenius plot, activation energy is – 0.088 eV. The maximum conductivity is found to be 311.79 S/cm at a particular temperature of 298 K. The conformed non-Debye type behavior in the MnO_2 materials is analyzed through modulus analysis and dielectric spectra. The modulus and dielectric spectra confirmed the relaxation process. Dielectric constant and dielectric loss were found from the dielectric spectral analysis. The dielectric constant was constant at high frequency region and varied at low frequency region. The dielectric constant is found to be – 1211 at a particular temperature of 298 K in very low frequency region. The dielectric loss also was constant at high frequencies in all temperature conditions and varied at low frequency region. Structure of MnO_2 nanoparticles has been analyzed by powder X-ray diffraction method. The powder XRD results revealed that the prepared nanoparticles sample was crystalline with a tetragonal phase. Average crystallite size is found to be around 20 nm using Scherrer formula.

Keywords: Nanoparticles, Microwave, Temperature, Impedance, Frequency.

DOI: 10.21272/jnep.12(3).03011 PACS numbers: 61.05.cp, 61.46.Df, 51.70. + f, 72.80.Jc, 72.80. – r

1. INTRODUCTION

Nanoparticles are measured and developed as 1 to 100 nm in size. In nanometer scale, particle size decreases and the surface area increases. As a result, the electromagnetic, thermal, mechanical and optical properties of nanoparticles have been modified. In last years, manganese dioxide (MnO_2) nanoparticles research has increased their characteristic chemical, physical properties and broad applications [1-3]. MnO_2 are known as very important semiconductors which have been studied in the past years due to technical and electrical importance. MnO_2 is a semiconductor oxide material having very nice band gap of 1.33 eV at normal room temperature. Due to the chemical and physical properties, MnO_2 has many applications. Manganese dioxides act as cathode materials for secondary batteries, and due to their catalysis and ion exchange reaction nature, they are used in magnetic resonance imaging (MRI). Nanosize particles and crystal morphology play many important roles in these applications, which has driven researchers to focus on the MnO_2 nanoparticles in recent years. The conductivity of MnO_2 nanoparticles is in good agreement with the properties of other materials [4-6]. MnO_2 takes place in different types of oxidation states, structural, and chemical forms. Distinctive properties and applications of manganese dioxide, the preparation of nanoparticles are investigated in order to study their structure, morphology and size under the control [7, 8]. Many effective approaches and methods have been used to synthesize MnO_2 nanomaterials by hydrothermal technique [9-12], sol-gel preparation method [13], wet chemical route method [14], microwave-assisted solution method [15], pulsed laser deposition technique [16] and precursor methods. The microwave-assisted solution technique is a simple preparation method that makes it easy to control the particle size. A good and perfect crystal will be widely distributed in all directions; therefore, many crystals are not perfect due to their finite size. This type of deviation from good size crystal leads to a broadening of the XRD peaks. The main properties explained from peaks height and width studies are the crystal size and lattice parameters. The crystal size of the nanoparticle is not the same as the particle size due to the formation of polycrystallites. Out of many applications, potential applications of good crystalline and semiconductor metal oxide materials are in good devices like as electrodes and batteries. Metal oxide crystals are difficult to prepare at low cost. MnO_2 nanoparticles in a crystalline form have become nanomaterials for some electronic (in future) devices due to their high dielectric responses. AC impedance spectroscopy technique has been widely used in few years, being a powerful tool for the study of the conductivity, electric modulus and dielectric studies.

2. MATERIALS AND METHODS

2.1 Materials

Manganese (II) sulphate ($MnSO_4$, AR grade), manganese oxalate (MnC_2O_4, AR grade) and sodium hydroxide (NaOH, AR grade) were used to prepare the nanoparticles. De-ionized water was used in this study.

2.2 Preparation of Manganese Dioxide Nanoparticles

The $MnSO_4$ and MnC_2O_4 salts were used to prepare MnO_2 nanoparticles using microwave-assisted solution technique. For instance, $MnSO_4$ and MnC_2O_4 were mixed with continuous stirring at a constant temperature of 40 °C at 60 min. During this process, sodium hydroxide solution was added to make the pH value 12. Stirring was continued for 60 min at a temperature of 40 °C. Then the stirring solution was kept in a microwave oven at a temperature of 30 °C for about 30 min and kept for 120 min for cooling. Synthesized brown precipitate was washed and filtered with de-ionized ethanol and water. Brown colored precipitates were dried for 72 h at normal temperature. The resultant powder was pressed into a pellet of 1 cm diameter and thickness of 0.448 mm using a hydraulic press for 10 min.

2.3 Instrumentation

It was found that in AC impedance spectroscopic studies, a computer controlled Zahner zennium IM6 meter was used within frequency range 10 μHz to 8 MHz at different temperatures. The powder XRD was characterized using XPERT-PRO spectroscopy using CuKα1 ($\lambda = 0.15$ nm) radiation. The prepared sample was scattered in the angle range of 2θ (10°-80°).

3. RESULTS AND DISCUSSION

3.1 AC Conductivity Spectra

The AC impedance spectroscopy method is a good technique for analyzing the electrical properties in the prepared nanomaterials. These measurements are separate individual contributions from various bulk materials and interfacial polarization taking place in the electrolyte, when stimulated by some external sinusoidal voltage. Fig. 1 shows the frequency dependent conductivity of manganese dioxide (MnO_2) as a function of different constant temperatures in a frequency range between 1 to 8 MHz. Conductivity (σ_{ac}) was measured using the relation: $\sigma_{ac} = \varepsilon_0\varepsilon_r\omega\tan\delta$, where ε_r is the relative permittivity and ω ($\omega = 2\pi f$) is the angular frequency. The conductivity arises due to hopping conduction mechanism [17]. Generally, frequency dependent conductivity can be expressed as $\sigma(\omega) = B(T)\omega^{s(T)}$; here, the first term is temperature dependent and the power of angular frequency will give information about hopping mechanism correlation. Conductivity of MnO_2 nanoparticles was calculated (temperature independent) in the temperature range from 298 K to 423 K.

From Fig. 1, conductivity increases exponentially with increasing frequency above 2.5 MHz. At very low frequencies, conductivity is non-varying at all operating temperatures, and it is varying at high operating temperatures. Fig. 2 shows the temperature dependence of conductivity between 298 K and 423 K. In this temperature range, electrical conductivity increases with decreasing temperature and agrees with the Arrhenius model: $\sigma_{ac} = \sigma_0\exp(-E_{ac}/kT)$, where σ_0 is a constant, k is the Boltzmann constant. The conductivity (σ_{ac}) of the prepared samples was investigated at different temperatures and is shown in Fig. 2. Fig. 2 illustrates the dependence between $\log\sigma_{ac}T$ vs $1000/T$ [18]. It was evident from the graph that, the conductivity increases with the decrease of operating temperatures. The lines of linear fit of the graph $\log\sigma_{ac}$ vs $1000/T$ obey the Arrhenius relationship $\sigma_{ac} = \sigma_0\exp(-E_{ac}/kT)$. Therefore, the sample exhibits the temperature range of investigation in conductivity behavior. The slopes of the above line plots ($E_a = -$ (slope)$\cdot k \times 1000$) have been found and estimated in activation energy [18]. The value of activation energy is -0.088 eV at a particular frequency of 5.5 MHz for MnO_2 nanoparticle.

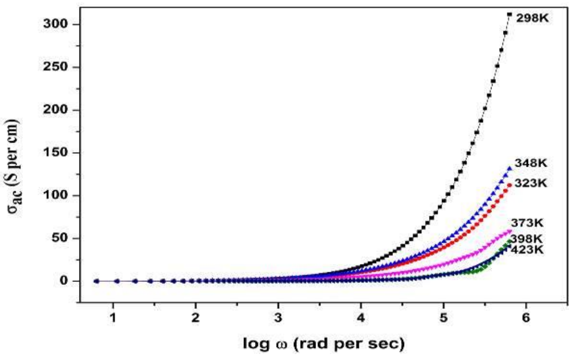

Fig. 1 – Conductivity spectra of manganese dioxide at different temperatures

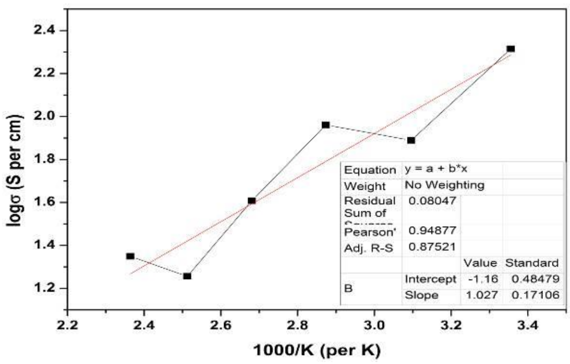

Fig. 2 – Arrhenius plot of manganese dioxide at different temperatures

3.2 Impedance Spectra

The pure MnO_2 nanoparticles were characterized using impedance spectroscopy. An impedance bridge (Zahner IM6) was used to measure the impedance in the frequency range of 1 to 8 MHz and the values are used for parallel RC circuit. The Cole-Cole plots depict the imaginary part of the impedance (Z'') versus the real part of the impedance (Z'). The electrical measurement was carried out at various temperatures. Fig. 3 shows the impedance spectra (Cole-Cole plot) of MnO_2 nanoparticles samples at various temperatures. The electrical properties of the materials were investigated using impedance analysis. Complex impedance is given as $Z^* = Z' - jZ''$

$$Z^* = \frac{Dj}{\omega^2 C^2},$$

where ω is the angular frequency, j is the imaginary root of -1, C is the capacitance of the sample, Z'' is the imaginary part of the impedance, Z' is the real part of the impedance, and D is the loss tangent.

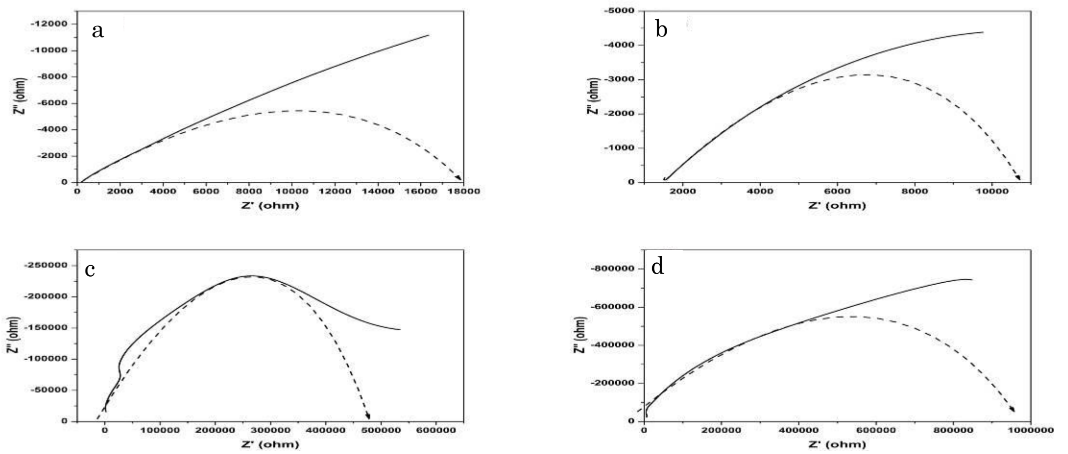

Fig. 3 – Cole-Cole plot of manganese dioxide nanoparticles at 298 K (a), 348 K (b), 398 K (c), 423 K (d)

The plots show that there is an inclined straight line in the low-frequency region at low temperatures of 298 K and 348 K. A single peak in the low-frequency region, which gives the information about the effect of blocking electrodes [20] followed by a partly semicircular arc, is in the high-frequency region. The real impedance axis lies above the center of the semicircle [19]. With increasing temperature, this stretch becomes normal and then it folds inward at temperatures side. This is due to the contribution of spatial charges and it is clearly observed in Fig. 3. A typical impedance spectrum of MnO_2 from 298 K to 423 K is also shown. Semicircles are partially observed on the high-frequency side, this is the response of the electrode (Bowen et al. 1999). Fig. 3 shows impedance spectra of MnO_2 at 398 K and 423 K. The low-frequency semicircle is due to the grain interior region and it is associated with that of the grain boundary area [20].

3.3 Modulus Spectra

In modulus representation, the total modulus properties are highlighted when its interfacial effects preserve to be abolished. So, complex modulus formations work to interrogate the reaction process present in the prepared MnO_2 nanoparticles. Real modulus (M') and imaginary modulus (M'') of the complex modulus (M^*) have been estimated for this technique. Fig. 4a shows the variation of M' versus logarithmic ω with various temperatures. M' value starts from zero at low frequency, confirming the presence of a nice electrode nature and M' values increased at higher frequencies [20], the frequency dispersion is observable at different surrounding temperatures (Fig. 4a). Variation of M'' versus logarithmic ω with various temperatures is presented in Fig. 4b. M'' value starts from zero at low frequencies and M'' values decreased at higher frequencies, the frequency dispersion is observable at different surrounding temperatures (Fig. 4b).

3.4 Dielectric Spectra

Analysis of dielectric spectra can be found using angular frequency versus ε' and ε''. The real part of dielectric ε' (dielectric constant) and the imaginary part of dielectric ε'' (dielectric loss) have been calculated using the formula of $\varepsilon^* = \varepsilon' + i{\cdot}\varepsilon''$. Fig. 5a, b show that, the ε' and ε'' decrease with increasing frequency, even though

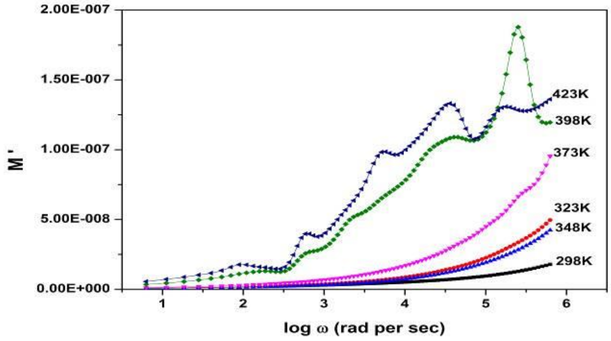

Fig. 4a – Logarithm of omega versus real part of the modulus of manganese dioxide nanoparticles at six different temperatures

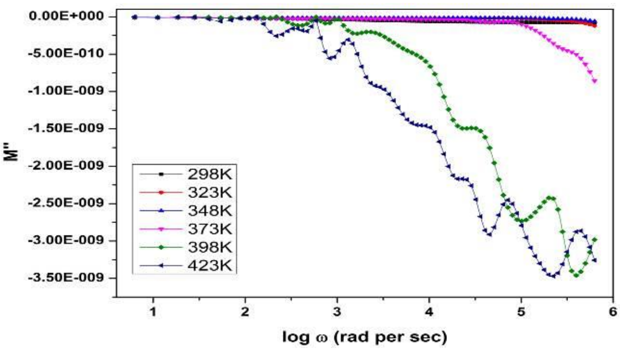

Fig. 4a – Logarithm of omega versus imaginary part of the modulus of manganese dioxide nanoparticles at six different temperatures

temperature decreases. Koop's concept and Maxwell-Wagner model (homogeneous double structure) [21] are used to give information about the dielectric properties of the semiconductor.

Conducting boundary is separated by poor conducting boundary and it is measured to be more successful at very high frequencies, while boundary is more successful at low frequencies from double structure model [22]. The dielectric constant decreases with decreasing temperature and logarithmic angular frequency. The dielectric loss also decreases with decreasing temperature and logarithmic angular frequency. MnO_2 nanoparticle has observed the dipolar relaxation from loss tangent as a function of temperature at different frequencies. Fig. 6 shows the dielectric relaxation peak for

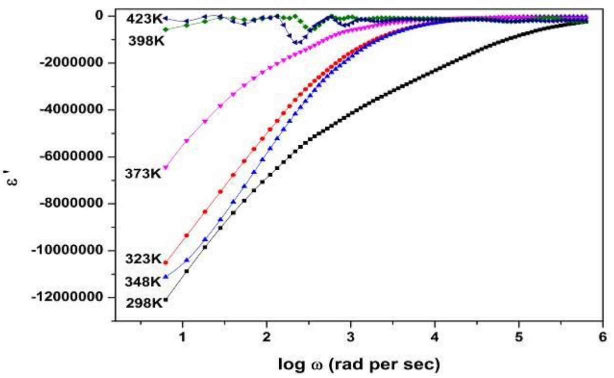

Fig. 5a – Logarithm of omega versus dielectric constant ε' of manganese dioxide nanoparticles at different temperatures

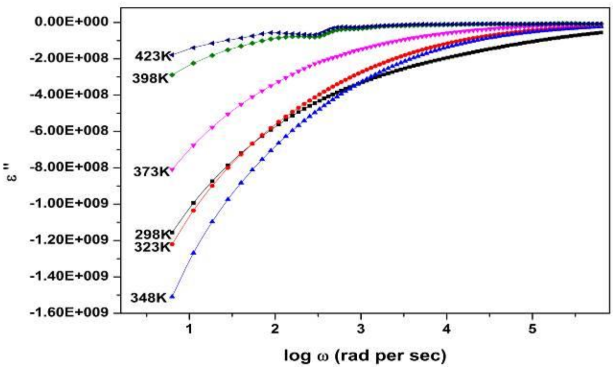

Fig. 5b – Logarithm of omega versus dielectric loss ε'' of manganese dioxide nanoparticles at different temperatures

MnO_2 nanoparticles at a frequency of 0, 1, 2, 3, 4 and 5 kHz. The temperature increase shows that the frequencies increase the relaxation peak shift toward the high temperature region. It is clear that the relaxation temperature may be caused by the moment of the chain dipole segment shown in Fig. 6.

3.5 XRD Spectra

XRD spectra for MnO_2 nanoparticles are shown in Fig. 7. All the observed peaks have been found as the (MnO_2 nanoparticle) tetragonal structure. Fig. 7 shows that, the diffraction peaks are very sharp at low Bragg angles, indicating the crystalline behavior. In Fig. 7, a very sharp diffraction peak with maximum height is seen at an angle of 28° and is followed by small sharp peaks. The crystalline size of the MnO_2 was calculated by the full width at half maximum method using Scherrer equation. The mean crystalline size is around 20 nm [23]. The peaks at 28°, 36°, 39°, 46°, 56°, 60°, 68° and 77° correspond to the Miller indices of (310), (400), (330), (321), (431), (521), (202) and (402), respectively, and represent the tetragonal structure of MnO_2. The lattice parameters of the unit cell are $a = 9.78$ Å and $c = 2.86$ Å and it is reported standard data JCPDS card number 44-0141.

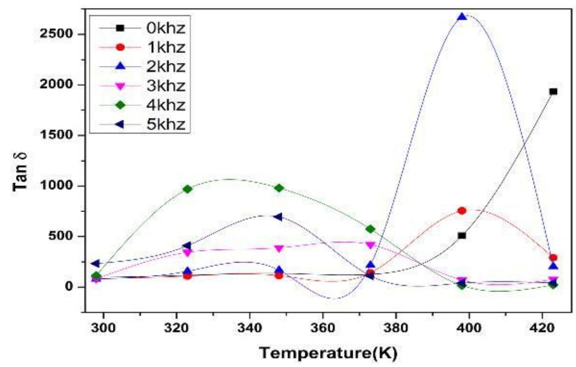

Fig. 6 – The dielectric relaxation peak for MnO_2 nanoparticles

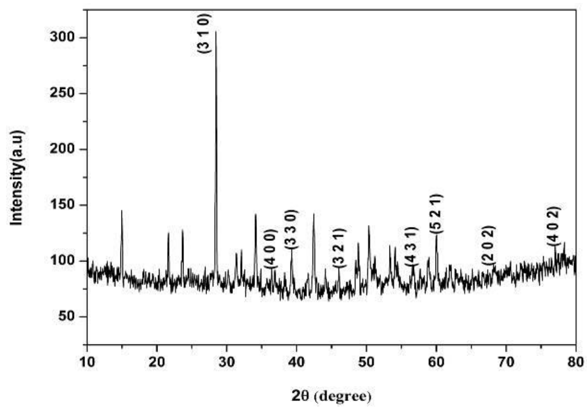

Fig. 7 – The XRD peaks for MnO_2 nanoparticles

4. CONCLUSIONS

The manganese dioxide nanoparticles have been successfully prepared by microwave-assisted solution method. Maximum conductivity has been observed for manganese dioxide at 298 K. The activation energy was calculated using the Arrhenius plot. MnO_2 nanoparticles have electrode material behavior; it was confirmed by impedance analysis and modulus spectra. The dielectric constants are high at higher temperature region and dielectric loss is also high at higher temperature region. The modulus spectra studies confirm the non-Debye behavior in the nanomaterials. The crystalline size and lattice parameters have been estimated by powder XRD technique.

ACKNOWLEDGEMENTS

The authors are thankful to authorities of JP College of Arts and Science, Agarakattu, Tenkasi for providing necessary research facilities.

REFERENCES

1. W.M. Li, J.K. Yuan, S.G. Mower, L.P. Xu, S. Sithambaram, M. Aindow, S.L. Suib, *Adv. Funct. Mater.* **16**, 1247 (2006).
2. J.A. Yan, E. Khoo, A. Sumboja, P.S. Lee, *ACS Nano* **4**, 4247 (2010).
3. M.S. El-Deab, T. Ohsaka, *Angew. Chem. Int. Ed.* **45**, 5963 (2006).
4. F. Rault, E. Pleyber, C. Campagne, M. Rochery, S. Giraud, S. Bourbigot, E. Devaux, *Polym. Degrad. Stab.* **94**, 955 (2009).
5. M.R. Johan, M.S.M. Suan, N.L. Hawari, H.A. Ching, *Int. J. Electrochem. Sci.* **6**, 6094 (2011).
6. R. Frick, B.M. Edenborn, A. Schlicker, B. Rothen-Rutishauser, D.O. Raemy, D. Guther, B. Hattendorf, W. Stark, B.B. Schimmer,

Toxicol. Lett. **205**, 163 (2011).
7. C. Wu, W. Xie, M. Zhang, L. Bai, J. Yang, Y. Xie, *Chem. Eur. J.* **15**, 492 (2009).
8. F.Y. Cheng, J.Z. Zhao, W. Song, C. Li, H. Ma, J. Chen, P. Shen, *Inorg. Chem.* **45**, 2038 (2006).
9. W. Xiao, D. Wang, X.W. Lou, *J. Phys. Chem. C* **114**, 1694 (2010).
10. G.L. Xu, Y.F. Xu, H. Sun, F. Fu, X.M. Zheng, L. Huang, J.T. Li, S.H. Yang, S.G. Sun, *Chem. Commun.* **48**, 8502 (2012).
11. D. Yan, P.X. Yan, G.H. Yue, J.H. Liu, J.B. Chang, Q. Yang, D.M. Qu, Z.R. Geng, J.T. Chen, G.A. Zhang, R.F. Zhuo, *Chem. Phys. Lett.* **440**, 134 (2007).
12. X. Wang, Y. Li, *Chem. Eur. J.* **9**, 300 (2000).
13. S.C. Vella Durai, R. Ganapathi Raman, E. Kumar, D. Muthuraj, *J. Nano- Electron. Phys.* **11** No 5, 05011 (2019).
14. N. Wang, X. Cao, L. He, W. Zhang, L. Guo, C. Chen, R. Wang, S. Yang, *J. Phys. Chem. C.* **112**, 365 (2008).
15. R. Anitha, E. Kumar, S.C. Vella Durai, *Asian J. Chem.* **31**, 1158 (2019).
16. X.Q. Yu, Y. He, J.P. Sun, K. Tang, H. Li, L.Q. Chen, X.J. Huang, *Electrochem. Commun.* **11**, 791 (2007).
17. E. Kumar, S.C. Vella Durai, L. Guru Prasad, D. Muthuraj, V. Bena Jothy, *J. Mater. Environ. Sci.* **8**, 3490 (2017).
18. G. Velciu, A. Melinescu, V. Marinescu, V. Fruth, C. Hornoiu, M. Preda, *Romanian J. Mater.* **49**, 173 (2019).
19. C.H. Hong, B.J. Park, H.J. Choi, *J. Colloid Interf. Sci.* **300**, 818 (2006).
20. C.R. Bowen, A.W. Tavernor, J. Luo, R. Stevens, *J. Eur. Ceram. Soc.* **19**, 149 (1999).
21. A.M.M. Farea, S. Kumar, J.K.M. Batoo, A. Yousef, C.G. Lee, J. Alimudden, *J. Alloy. Compd.* **464**, 361 (2008).
22. K.M. Batoo, S. Kumar, C. Lee, Alimuddin, *Curr. Appl. Phys.* **9**, 1397 (2009).
23. S.C. Vella Durai, E. Kumar, D. Muthuraj, V. Bena Jothy, *Int. J. Nano Dimens.* **4** No 4, 410 (2019).

Дослідження електричних та структурних властивостей наночастинок діоксиду марганцю

S.C. Vella Durai[1], E. Kumar[2], D. Muthuraj[3], V. Bena Jothy[4]

[1] *Department of Physics, JP College of Arts and Science, Agarakattu, Tenkasi, Tamilnadu, India*
[2] *School of Science, Department of Physics, Tamil Nadu Open University, Chennai. Tamilnadu, India*
[3] *PG and Research Department of Physics, The M.D.T Hindu College, Tirunelveli. Tamilnadu, India*
[4] *Department of Physics & Research Center, Women's Christian College, Nagarcoil. Tamilnadu, India*

Кристалічний діоксид марганцю (MnO_2) готували методом розчинення в мікрохвильовій печі з використанням гідроксиду натрію як агента. Електропровідність, електричний модуль та діелектричні властивості наночастинок MnO_2 були проаналізовані методом імпедансної спектроскопії в діапазоні частот від 1 до 8 МГц та діапазоні температур від 273 до 423 К. Провідність MnO_2 зростає зі збільшенням частоти. Було встановлено, що температурна залежність провідності наночастинок підкоряється діаграмі Арреніуса, енергія активації становить – 0,088 еВ. Максимальна провідність виявляється рівною 311,79 См/см при конкретній температурі 298 К. Відповідна не дебаєвська поведінка у матеріалах MnO_2 аналізується за допомогою аналізу модулів та діелектричних спектрів. Модульний і діелектричний спектри підтвердили процес релаксації. Діелектрична константа та діелектричні втрати були виявлені діелектричним спектральним аналізом. Діелектрична константа була постійною в області високих частот і варіювалася в області низьких частот. Діелектрична константа виявилася рівною – 1211 при певній температурі 298 К в області дуже низьких частот. Діелектричні втрати також були постійними при високих частотах в будь-яких температурних умовах і змінювались в області низьких частот. Структуру наночастинок MnO_2 проаналізували методом порошкової рентгенівської дифракції. Результати порошкової рентгенографії показали, що підготовлений зразок наночастинок був кристалічним з тетрагональною фазою. За формулою Шеррера середній розмір кристалітів становить близько 20 нм.

Ключові слова: Наночастинки, Мікрохвильова піч, Температура, Імпеданс, Частота.